John von Neumann Institute for Computing

Soft Matter- and Nano-Systems: Computer Simulations

F. Bürzle, K. Franzrahe, P. Henseler, Ch. Schieback,
M. Dreher, J. Neder, W. Quester, D. Mutter,
M. Schach, P. Nielaba

published in

NIC Symposium 2008,
G. Münster, D. Wolf, M. Kremer (Editors),
John von Neumann Institute for Computing, Jülich,
NIC Series, Vol. **39**, ISBN 978-3-9810843-5-1, pp. 245-252, 2008.

http://www.fz-juelich.de/nic-series/volume39

Soft Matter- and Nano-Systems: Computer Simulations

Florian Bürzle, Kerstin Franzrahe, Peter Henseler, Christine Schieback, Markus Dreher, Jörg Neder, Wolfram Quester, Daniel Mutter, Margit Schach, and Peter Nielaba

Physics Department, University of Konstanz, 78457 Konstanz, Germany
E-mail: {firstname.surname}@uni-konstanz.de

Soft matter systems have been investigated by Monte Carlo and Brownian Dynamics simulations. In particular the behaviour of two dimensional binary hard disk mixtures in external periodic potentials has been studied as well as the transport of colloids in micro-channels and the features of proteins in lipid bilayers. Ni nanocontacts have been analyzed by Molecular Dynamics simulations with respect to their conductance and structural properties under stretching. The properties of Si clusters in external fields have been computed by density functional methods, and static and dynamic properties of magnetic model systems by the Landau-Lifshitz-Gilbert equation. In the following sections an overview will be given on our recent results.

1 Two-Dimensional Model Colloids in External Periodic Fields

In monolayers on crystalline surfaces one can observe an intricate competition between effects due to the interaction of components within the layer and those with the underlying substrate.

Such complicated experimental systems can be modelled by two-dimensional colloidal systems. The interactions within the monolayer can be altered by changing the interaction potential of the colloids, while the shape and strength of the substrate potential can be modelled by external light fields. The advantage of the model system is, that via laser scanning microscopy direct access to the particle configurations is given. In this way it is possible to gain insight in the relative importance of the various possible physical processes that occur. From the theoretical point of view, even the relatively simple combination of a monodisperse system in a one-dimensional, spatially periodic light field shows a highly non-trivial phase behaviour as the amplitude of the external field is raised: Laser Induced Freezing (LIF) and Laser Induced Melting (LIM).

The interesting LIF- and LIM- effects have been studied in the HPC project by Monte Carlo simulations in two dimensions using commensurate[1,2] and incommensurate potentials. In addition, interesting ordering phenomena of two-dimensional colloidal crystals confined in strips of finite widths have been analysed by MC simulations[3,4].

In particular we explored[5] a hard disk system with commensurability ratio $p = \sqrt{3}a_s/(2\lambda) = 2$, where a_s is the mean distance between the disks and λ the period of the external potential. Three phases, the modulate liquid, the locked smectic and the locked floating solid have been observed, in agreement with other experimental[6] and analytical[7] studies. Various statistical quantities like order parameters, their cumulants and response functions, have been used to obtain a phase diagram for the transitions between these three phases.

For our analysis, we consider a system of hard disks with diameter σ. This system is

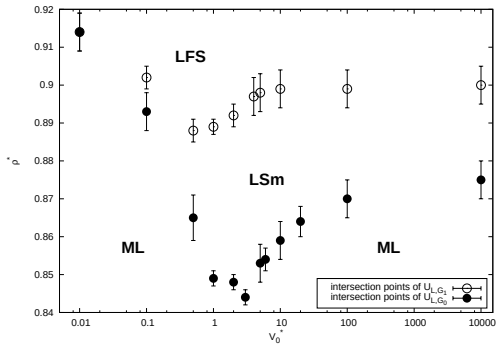

Figure 1. Phase diagram in the ρ^*/V_0^* plane. Transitions points have been obtained by considering order parameter cumulant intersection points.

subjected to an external potential

$$V(x,y) = V_0 \sin\left(\frac{2\pi}{\lambda}x\right) \tag{1}$$

Our system is characterized by the reduced density $\varrho^* = \varrho\sigma^2$ and the reduced potential strength $V_0^* = V_0/(k_B T)$, where k_B is the Boltzmann constant and T the temperature. For simplification, σ was set to unity in our simulation.

The resulting phase diagram shown in Fig. 1 was obtained by using the data from the cumulant intersection points. As the most important result, we see that the melting curves for both order parameters show a distinct remelting behaviour at higher V_0^*, as was expected by the theory of Radzihovsky *et al.*[7]. The melting curve from LFS to LSm (open circles) resembles those obtained by Strepp *et al.*[1] for $p = 1$ quite well. The other transition curve from ML to LSm (closed circles) shows that here the global minimum of the curve is slightly shifted to higher potential strengths. Also the minimum is located at considerable lower densities. Finally, it must be emphasized that at $V_0^* \to 0$, the different melting curves collapse into one single curve, as is expected for physical reasons.

In the studies of bi-disperse colloidal crystals our emphasis lies on the analysis of their structural and elastic properties. Monte Carlo simulations are an effective means for such analysis. We are interested in the dependence of these properties on the mixing ratio and size ratio of the components[8]. Monte Carlo simulations for hard disk mixtures with different diameter ratios σ_B/σ_A have been performed in the NPT- and NVT- ensemble in order to analyze the structural properties and phase transition parameters. Another point of interest is the phase behaviour of such systems in external, periodic light fields[9]. A bi-disperse hard disk mixture (mixing ratio 50% and diameter ratio $\sigma_B/\sigma_A = 0.414$) was exposed to an one dimensional, spatially periodic external light field. The wavelength of the external field was chosen to be commensurate to the square lattice, which yields the highest packing fraction for the given mixture. The commensurability ratio was set to $p = 2$. In these studies one has to distinguish between three cases: (I) only the smaller component interacts with the external field, (II) both components interact with the field and (III) only the larger component interacts with the field.

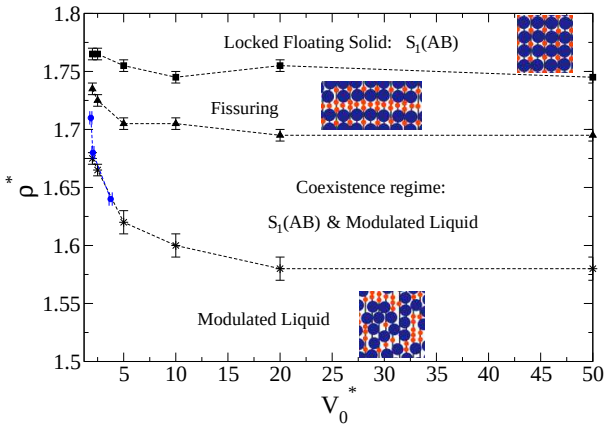

Figure 2. The $\varrho^* - V_0^*$ plane of the phase diagram of an equimolar binary mixture ($\sigma_B/\sigma_A = 0.414$) for the case, when only the smaller component interacts with the external light field.

Figure 2 shows[9] the phase diagram obtained for case (I). It was calculated by lowering the dimensionless number density $\varrho^* = \varrho\sigma_A^2$ and taking a commensurate path through phase space, meaning the wavelength of the external field $\lambda = 1/(\sqrt{2\varrho^*})$ changes with ϱ^*. Part of the phase diagram was obtained by raising the potential strength V_0^* at constant ϱ^*. Simulations carried out in an incommensurate setting, i.e. λ is kept constant independent of ϱ^*, intersect the phase diagram consistently.

At low external fields ($V_0 \leq 1.5$) we observe a laser induced coexistence of a triangular lattice of the larger component with a smaller component enriched binary fluid. In the field free case the system does not expose phase separation. This phase separation is driven by the attempts of the smaller components to form chains along the minima of the external field. Case (II) and (III) also show a laser induced de-mixing at low potential strengths. In these cases the larger component interacts directly with the external field. The phase separation is now also driven by the attempt of the larger component itself to align with the minima of the external field. The resulting coexisting monodisperse solid is a rhombic, commensurate lattice.

At higher external fields as shown[9] in figure 2 case(I), i.e. only the smaller component interacts with the external field, exhibits a laser induced freezing transition into the the commensurate $S_1(AB)$ square lattice. Depending on the overall density ϱ^* the $S_1(AB)$ locked floating solid is either in the one phase regime or coexists with an equimolar binary fluid. These two regimes are separated by a fissuring region, in which the smaller component is free to move perpendicular to the minima of the external field.

2 Transport of Colloids in Micro-Channels

We conducted Brownian dynamics (BD) simulations of a two-dimensional microchannel[10] setup in order to investigate the flow behaviour of the colloidal particles within the channel systematically for various parameter values of constant driving force, overall particle density, and channel width. The pair interaction $V(r) = (\mu_0/4\pi)M^2/r^3$ (M is the dipole

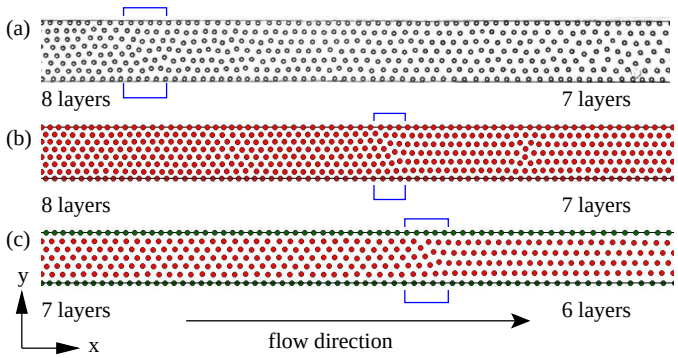

Figure 3. (a) Video microscopy snapshot of colloidal particles moving along the lithographically defined channel. (b) Simulation snapshots for a channel ($692 \times 60\mu m$, $\Gamma \approx 2.5$) with ideal hard walls ($573.3 \times 45\mu m$, $\Gamma = 115$), (c) the same as in (b) with the particles at the walls (marked green) kept fixed ($573.3 \times 45\mu m$, $\Gamma = 902$). The blue rectangles mark the layer transition region.

moment) is purely repulsive and can be characterized by the dimensionless interaction strength $\Gamma = \mu_0 M^2 \rho^{2/3}/(4\pi k_B T)$.

Particles are confined to the channel by ideal elastic hard walls in y-direction and at $x = 0$ (channel entrance). Also we performed simulations with the particles at the wall kept fixed. The channel end is realized as an open boundary. To keep the overall number density in the channel fixed, every time a particle leaves the end of the channel a new particle is inserted at a random position (avoiding particle overlaps) within the first 10% of the channel, acting as a reservoir. A cutoff of 10σ was used along with a Verlet next neighbour list[11]. Checks of particle overlaps are included in the simulation, but for all ordered systems we never found two overlapping particles.

A typical snapshot from the experiment[10] of the particles moving along the channel is shown in Fig. 3(a). Similar snapshots we get from simulations[10] with co-moving (Fig. 3(b)) and fixed boundary particles (Fig. 3(c)), i.e., the velocity is kept to zero for the particles at the channel wall. In most regions of the channel the particles are placed in a quasi-crystalline order. This behaviour is due to the strength of the particle interactions caused by the external magnetic field (high Γ-values), which leads to quasi-crystalline behaviour in unbounded systems as well. The formation of this order naturally gives rise to the formation of layers in the motion of the particles along the channel. A similar layering phenomenon has been observed in channels under equilibrium condition[12]. Additionally to this layer formation we observe, both in experiment and in simulation, a decrease of the number of layers in the direction of motion. In between both regions therefore a region exists in which the particles cannot be well-ordered. This region is called the layer-reduction zone. In Fig. 3 these regions have been marked.

The reduction of the number of layers originates from a density gradient along the channel. The local particle density inside the channel is shown in Fig. 4(a) and (b) together with the particle separations in x- and y-directions. In the experiment (Fig. 4(a)) the density decreases monotonically along the direction of the motion of the particles by about 20%. The average density in the channel shows fluctuations on the order of 10% as a function of time. The total increase in density, however, is less than 3% during the total time of

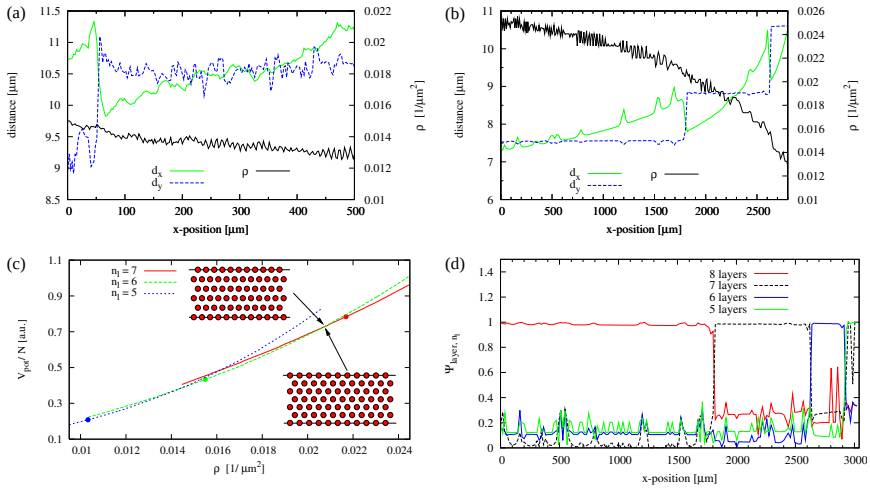

Figure 4. Local lattice constants d_x and d_y and local particle density (a) in the experiment and (b) in the BD simulation. The results are obtained for the systems of Fig. 3(a) and (b) respectively. (c) Potential energies per particle of different layer configurations as a function of the particle density. The dots mark the perfect triangular lattices for 5, 6 and 7 layers. Also shown are parts of the configurations with 7 and 6 layers at the intersection point. (d) Plots of the layer order parameter for the configuration snapshot of Fig. 3(b).

the experiment. We therefore argue that the density gradient is formed in a quasi-static situation. This argument is confirmed by results of BD simulations (Fig. 4(b)), where the corresponding decrease of the particle density is observed.

3 Conductance and Structural Properties of Ni Nanocontacts

During the last years a lot of attention has been devoted to the analysis of contacts of magnetic materials. In these nanowires the spin degeneracy is lifted, which can potentially lead to interesting spin-related phenomena in the transport properties.

Here we address the issue of the conductance quantization and the spin polarization of the current of Ni contacts. We have combined classical molecular dynamics simulations of the breaking of nanocontacts with conductance calculations based on a tight-binding model.[13,14] For Ni we have applied our method to a Hamiltonian with spin-dependent matrix elements.[15]

We analyzed the evolution of the conductance during the formation of a Ni dimer structure, which is the most common geometry in the last stages of the breaking process. In addition to the evolution of the conductance and transmission eigenchannels for both spin components separately, we computed the MCS radius, the strain force, and the spin polarization of the current, which is defined as $P = (G^{\uparrow} - G^{\downarrow})/(G^{\uparrow} + G^{\downarrow}) \times 100\%$, where G^{σ} is the conductance of the spin component σ. Here, spin up ($\sigma = \uparrow$) means majority spins and spin down ($\sigma = \downarrow$) minority spins. In the last stages of the stretching the conductance for the majority spins lies below $1.2e^2/h$ and is dominated by a single channel, while for the minority spin there are still up to four open channels and the conductance is close to $2e^2/h$, adding up to a total conductance of around 1.2–$1.6G_0$.

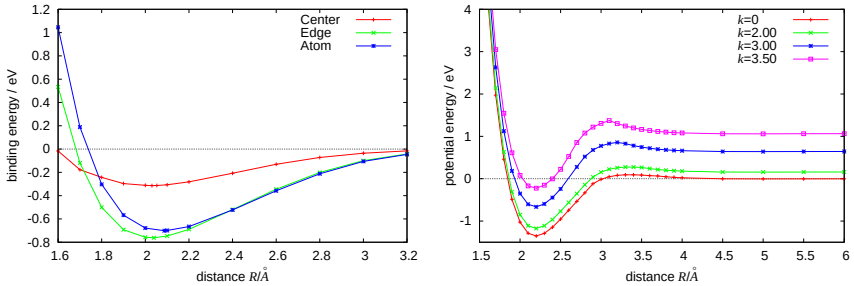

Figure 5. Left: Binding energy of Si atoms as function of distance over certain sites of a graphite surface Right: Potential energy for two Si_4 clusters as function of distance in an external parabolic potential.

For ferromagnetic Ni, we have shown that the contacts behave as a mixture of a noble metal (such as Ag) and a transition metal (such as Pt). While the $4s$ orbitals play the main role for the transport of the majority-spin electrons, the conduction of the minority-spin electrons is controlled by the partially occupied $3d$ orbitals. This follows from the position of the Fermi energy, which lies in the s band for the majority spins and in the d bands for the minority spins. Our results indicate the absence of any conductance quantization, and show how the spin polarization of the current evolves from negative values in thick contacts to even positive values in the tunneling regime after rupture of the contact.

4 Si_n Clusters, Magnetic Model Systems and Membranes under Tension

We computed the properties of selected Si_n clusters approaching each other and the effect of external fields and surfaces[17,18] by DFT methods[19].

One example shown here is the approach of Si-atoms to a graphite surface. The resulting binding energy as function of distance over certain sites[16] is shown in Fig. 5. It follows that the site above the C-C bonds is energetically preferred. Another example[18] is the effect of an external parabolic potential, $V(x, y, z) = k^2y^2$ on the potential energy of two Si_4 clusters as a function of distance, s. Fig. 5. Two nearest atoms of the two clusters are fixed at a distance R, the other atoms are allowed to move freely. For increasing k values the potential energy develops a fusion barrier at a distance of about 3 Å.

Using the Heisenberg Hamiltonian and the Landau-Lifshitz-Gilbert equation interesting insight into the behaviour of domain walls in confined geometry at finite temperature has been computed[20–22].

The dynamics of the spin reversal processes in systems with moments attached to caps of (colloidal) spheres have been computed[22] for different system sizes and external magnetic fields. Fig. 6 shows the hysteresis effect of external magnetic fields at angle ϑ relative to the x-axis.

Lipid bilayers and incorporated proteins form biological membranes. These barriers define the inside and the outside of a cell and are indispensable for live. Usually the microscopic surface tension of membranes is small or vanishes altogether. One aim of our work[23] is to study the effect of an applied tension to a model bilayer, unsing the lipid

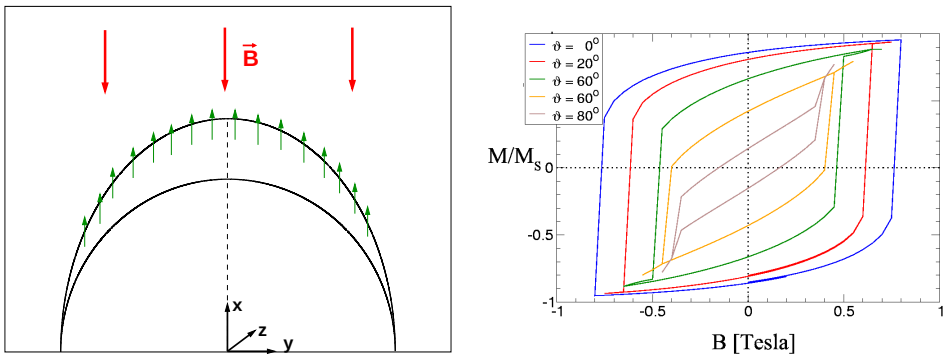

Figure 6. Left: Sketch of the geometry; Right: Hysteresis for different angles ϑ relative to the x-axis. The caps have a diameter of 48 nm and a height of 12 nm.

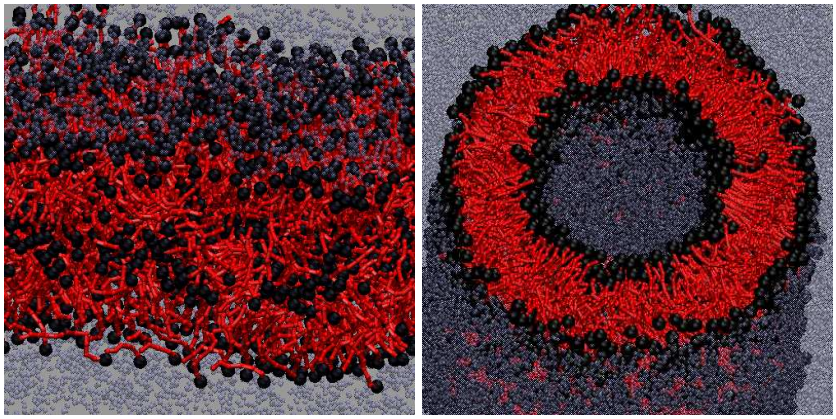

Figure 7. Left: Snapshot of a double bilayer configuration; Right: Tether consisting of 4,800 lipids

model of Ref.[24,26]. Does this tension cause a change in the behaviour of incorporated model proteins, e.g. lead to an increasing lipid mediated attraction or repulsion between two proteins?

Other points of interest in our project are the examination of membrane multi layers (Fig. 7) and tethers (Fig. 7) within and without an applied tension, respectively. These configurations[23] require high computing capacities due to the system size. The shown tether, e. g., consists of 4800 lipids and more than 90,000 solvent particles. The program has been parallelized and technical details about that can be found in Ref.[25].

Acknowledgments

We gratefully acknowledge useful discussions with K. Binder, C. Cuevas, F. Pauly, F. Schmid, S. Sengupta, B. West, support from the SFB 513, the SFB TR6 and the SFB 767 and granting of computer time from the NIC.

References

1. W. Strepp, S. Sengupta, P. Nielaba, Phys. Rev. **E63**, 046106 (2001).
2. P. Nielaba, W. Strepp, S. Sengupta, in *Computer Simulations in Condensed Matter: From Materials to Chemical Biology*, edited by M. Ferrario, G. Ciccotti, K. Binder, Springer, Berlin, pp.163 (2006).
3. A. Ricci, P. Nielaba, S. Sengupta, K. Binder, Phys. Rev. **E74**, 010404 (R) (2006).
4. A. Ricci, P. Nielaba, S. Sengupta, K. Binder, Phys. Rev. **E75**, 011405 (2007).
5. F. Bürzle, P. Nielaba, Phs. Rev. **E76**, 051112 (2007).
6. J. Baumgartl, M. Brunner, C. Bechinger, Phys. Rev. Lett. **93**, 168301 (2004).
7. E. Frey, D.R. Nelson, L. Radzihovsky, Phys. Rev. Lett. **83**, 2977 (1999); L. Radzihovsky, E. Frey, D.R. Nelson, Phys. Rev. **E63**, 031503 (2001).
8. K. Franzrahe, P. Henseler, A. Ricci, W. Strepp, S. Sengupta, M. Dreher, Chr. Kircher, M. Lohrer, W. Quester, K. Binder, P. Nielaba, Comp. Phys. Commun. **169**, 197 (2005).
9. K. Franzrahe, P. Nielaba, Phys. Rev. **E**, in press.
10. M. Köppl, P. Henseler, A. Erbe, P. Nielaba, and P. Leiderer. Phys. Rev. Lett. **97**, 208302 (2006).
11. M. P. Allen and D. J. Tildesley. *Computer Simulation of Liquids* (Oxford Science Publications, 1987).
12. R.Haghgooie, C.Li, P.Doyle, Langmuir**22**, 3601 (2006).
13. F. Pauly, M. Dreher, J.K. Viljas, M. Häfner, J.C. Cuevas, and P. Nielaba, Phys. Rev. B **74**, 235106 (2006).
14. M. Dreher, F. Pauly, J. Heurich, J.C. Cuevas, E. Scheer, and P. Nielaba, Phys. Rev. B **72**, 075435 (2005).
15. See parameters ni_ferro_par at `http://cst-www.nrl.navy.mil/bind/ni.html`; M.I. Haftel, N. Bernstein, M.J. Mehl, and D.A. Papaconstantopoulos, Phys. Rev. B **70**, 125419 (2004).
16. W. Quester, Dissertation, U. Konstanz (in preparation).
17. F. von Gynz-Rekowski, W. Quester, R. Dietsche, Dong Chan Lim, N. Bertram, T. Fischer, G. Ganteför, M. Schach, P. Nielaba, Young Dok Kim, Eur. Phys. J. **D**, in press.
18. M. Schach, Diplomarbeit, U. Konstanz (2007).
19. CPMD. Copyright IBM Corp 1990–2001, Copyright MPI für Festkörperforschung Stuttgart 1997–2004. `http://www.cpmd.org/`.
20. C. Schieback, M. Kläui, U. Nowak, U. Rüdiger, P. Nielaba, Eur. J. **B**, in press.
21. D. Backes, C. Schieback, M. Kläui, F. Junginger, H. Ehrke, P. Nielaba, U. Rüdiger, L.J. Heyderman, C.S. Chen, T. Kasama, R.E. Dunin-Borkowski, C.A.F. Vaz, J.A.C. Bland, Appl. Phys. Lett. **91**, 112502 (2007).
22. D. Mutter, Diplomarbeit, U. Konstanz (2007).
23. J. Neder, Dissertation, U. Konstanz (in preparation).
24. O. Lenz and F. Schmid, J. Mol. Liq. **117**, 147 (2005).
25. F. Schmid, D. Düchs, O. Lenz, B. West, Comp. Phys. Commun. **177**, 168 (2007).
26. O. Lenz and F. Schmid, Phys. Rev. Lett. **98**, 058104 (2007).